

Drift Demand Predictions in Low to Moderate Seismicity Regions

E. Lumantarna¹, M. Fardipour¹, K. Thinley¹, K. Cao¹, N. Lam¹ and , J. Wilson²

1. Dept of Civil and Environmental Engineering, The University of Melbourne, Parkville, VIC 3010, Australia.

2. School of Engineering and Industrial Science, Swinburne University of Technology, Hawthorne, VIC 3122, Australia.

ABSTRACT

This paper presents results obtained from a recent study which is aimed at assessing the drift demand on buildings of different height ranges for projected earthquake scenarios in Australia. Parametric studies of tall buildings have been carried out based on modal analysis. Important parameters defining the response behaviour of buildings including building height, structural configurations and form of construction have been collated from recent field survey reports. The estimated drift demands can be compared with the limiting drift capacity to enable various levels of damage to be predicted for given earthquake scenarios, building types and site classes.

1 Introduction

The displacement demand on a structure can become insensitive to its natural period. This can happen if the natural period of the structure has reached or exceeded the dominant period of the applied excitations as illustrated by the displacement response spectrum of Figure 1 (which shows the response of the structure to a single pulse or a series of periodic pulses). In earthquake scenarios that are generated by rupture of up to M7 and are consistent with a design peak ground velocity of 50 – 100 mm/s on rock, the dominant period of excitations is considered to be up to 1.5 s for both rock and soil sites. Structures are subject to limited peak displacement demand in such conditions.

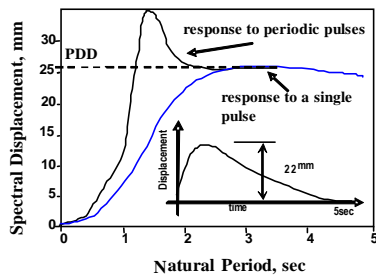


Figure 1 Displacement-controlled behaviour (Lam & Chandler, 2005)

In this study, the displacement controlled phenomenon is used as the basis for estimating the maximum displacement demand on structures including non-ductile structures (Lumantarna et al. 2007, Bhamare et al., 2008, Lumantarna et al., 2009) and structures which possess significant asymmetry on plan (Lumantarna et al., 2008). The developed methodology is simple to apply in that the maximum displacement demand of the structure is constrained by the peak displacement demand (PDD) which is the peak level of an elastic response spectrum for 5% damping. The PDD value is a function of the frequency content and intensity of ground shaking. Consequently, reasonable estimates of the maximum displacement (drift) demand on the structure can be made without prior knowledge of its natural period (which is well known to be difficult to predict with good accuracies).

In this paper, the developed methodology has been extended to the estimation of the maximum drift demand in tall buildings. The peak displacement demand of linear elastic systems associated with the seismic hazard of Australia as stipulated in the Australian Standard (AS1170.4, 2007) is first presented (Section 2). A model for predicting the drift demand on tall buildings was developed from modal analysis results (Section 3). The methodology has been further developed to account for inelastic behaviour of the building (Section 4). Results from these investigations have been integrated with other information to develop a simple assessment procedure for practical applications (Section 5). The research project is aimed at enabling the state of damage to a range of infrastructure to be predicted for given earthquake scenarios and site conditions.

2 Peak Displacement Demand

The maximum displacement demand of elastic SDOF systems can be obtained directly from an elastic displacement response spectrum. Figure 2 presents the displacement response spectrum of the idealized bi-linear form. The displacement response spectrum is

defined by two parameters: maximum displacement response spectral displacement (RSD_{max}) and second corner period (T_{corner}).

The value of RSD_{max} on rock sites as per the Australian Standard of Seismic Actions AS1170.4 (2007) can be estimated by Eq (1):

$$RSD_{max} = 1.8(750R_p Z)F_v \frac{T_{corner}}{2\pi} \quad (1)$$

where, Z is the seismic hazard factor, R_p is the return period factor (which is normalized to unity for return period of 500 years), F_v is the site amplification factor (which is normalized to unity for average rock conditions). T_{corner} is the second corner period (Lam et al., 2000) at which the linear part of the response spectrum intercepts the constant (flat) part of the response spectrum (Figure 2). The Australian Standard stipulates an onerous second corner period (T_{corner}) value of 1.5 seconds.

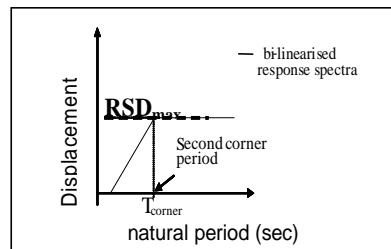


Figure 2 Bi-linearized model of displacement response spectrum

Values of RSD_{max} that are consistent with the stipulations of AS1170.4 (2007) are defined by Eq (1). The estimated RSD_{max} values for 500 and 2500 year return period earthquakes is presented in Table 1.

Table 1 Estimates of RSD_{max} (mm) for Australian conditions

Site	F_v	500 yr RP ($k_p = 1.0$)				2500 yr RP ($k_p = 1.8$)			
		$Z = 0.06$	$Z = 0.08$	$Z = 0.10$	$Z = 0.12$	$Z = 0.06$	$Z = 0.08$	$Z = 0.10$	$Z = 0.12$
Class B	1.0	19	26	32	39	35	46	58	70
Class C	1.4	27	36	45	54	49	65	81	97
Class D	2.25	44	58	73	87	78	104	131	157
Class E	3.5	68	90	113	135	122	162	203	244

Note: K_p is the probability factor for the annual probability of exceedance, appropriate for the limit state under consideration according to Australian Standard (AS1170.4, 2007)

3 Drift Demand on Tall Buildings

3.1 Parametric Studies

The maximum drift demand on tall buildings can be estimated by modal analysis or by elastic time-history analysis if linear elastic behaviour is assumed. An elastic dynamic analysis program has been developed on EXCEL spreadsheet (Lam et al., 2009). The developed spreadsheet analyses the building as a cantilever column element (which has point masses lumped at every storey level) to represent the behaviour of lateral resisting elements namely structural walls and moment frames. The developed spreadsheet has the capability to simulate the dynamic behaviour of tall buildings which are jointly supported by these two types of elements.

In the parametric studies of multi-storey buildings the analytical models were divided equally into 10 levels with point masses lumped on each level as shown schematically in Figure 3. It should be noted that each level can represent more than one-storey in the building. For example: the building model with 10 levels could actually represent the dynamic behaviour of a 30-storey building with three stories lumped at each level. The distribution of mass up the height of the building was assumed to be uniform. The lateral stiffness of the building has been calibrated in order that the calculated natural period of vibration is consistent with recommendations presented in AS1170.4 (2007). Wind loading often governs the design of multi-storey buildings in regions of low to moderate seismicity. The assumed variation of the lateral stiffness of the building up its height has been summarized in Table 2. The assumptions were based on the strength demand on the walls by wind loads as stipulated by AS1170.2 (2002).

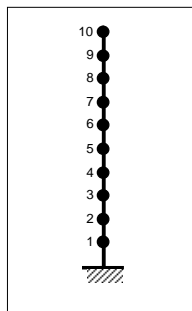
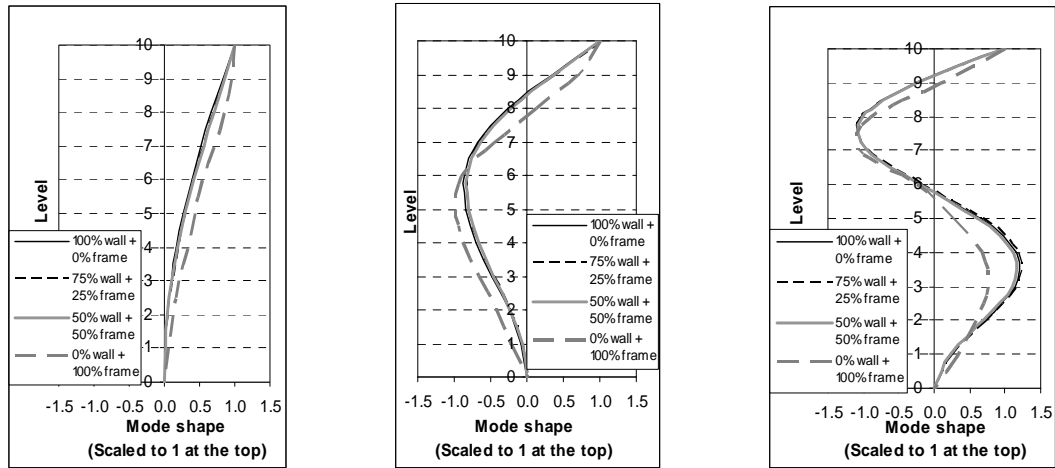


Figure 3 Multi-storey building model

Table 2 Distribution of lateral stiffness along the height of building

Level	Height of building (m)			
	< 30	30 - 40	40 - 70	>70
10	0.5	0.25	0.25	0.25
9	0.5	0.25	0.25	0.25
8	0.5	0.25	0.25	0.25
7	0.5	0.25	0.25	0.25
6	0.5	0.25	0.5	0.5
5	0.5	0.5	0.5	0.5
4	0.5	0.5	0.5	0.75
3	1	1	0.75	0.75
2	1	1	1	1
1	1	1	1	1

Sensitivity analyses were undertaken to investigate the interaction between structural walls and moment frames in tall buildings and their effects on their displacement response behaviour. In a sensitivity analysis the values of **EI** (and **GA**) which represent the flexural stiffness of structural walls (and the shear rigidity of moment frames) were varied to represent different degrees of contribution from the moment frames (which varied between 0% and 100%). Typical mode shapes from the first three modes of vibration are presented in Figure 4. Interestingly, the modal displacements were found to be insensitive to variations in the percentage contribution by the moment frames. The rest of the analyses presented in this paper were based on multi-storey building models which is fully flexural in nature (ie. 0% contribution from the moment frames).



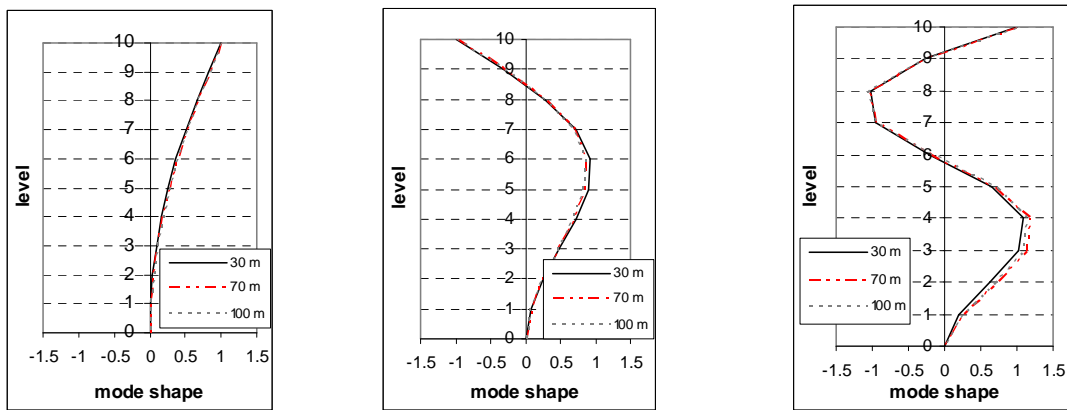
(a) mode shape 1

(b) mode shape 2

(c) mode shape 3

Figure 4 Mode shapes of multi-storey buildings with varying wall-frame contribution

Further analyses have been undertaken to investigate the effects the height of the building has upon its displacement response behaviour. In the sensitivity analysis the building height was varied from 20 m to 150 m and the lateral stiffness was distributed according to the ratios shown in Table 2. It was found from the analyses that the modal displacements for the first three modes of vibration were not sensitive to the height of the building (Figure 5). Generic mode shapes (Figure 6) could hence be used for estimating the maximum drift demand.



(a) mode shape 1

(b) mode shape 2

(c) mode shape 3

Figure 5 Mode shapes of multi-storey buildings with varying height

3.2 Estimation of drift demands

The maximum angle of drift θ_{\max} is related to the average drift angle θ_{ave} by the following equation:

$$\theta_{\max} = \lambda_{\max} \theta_{\text{ave}} \quad (2)$$

where, λ_{\max} is the maximum drift angle amplification factor.

The average drift angle is shown schematically in Figure 7 and is defined by:

$$\theta_{ave} = \Delta_{max}/H \quad (3)$$

where, H is the total height of the building. Δ_{max} is the maximum displacement at the top of the building attributed to the fundamental mode of vibration as defined in the following:

$$\Delta_{max} = \phi_{10,1} \mathbf{PF}_1 \mathbf{RSD}(T_1) \quad (4)$$

$\phi_{10,1}$ is the modal displacement at level 10 of the first mode of vibration (Figure 6), \mathbf{PF}_1 is the participation factor and $\mathbf{RSD}(T_1)$ is the response spectral displacement at the fundamental natural period of vibration T_1 . The modal participation factors were calculated for the three vibration modes and were based on mode shape vectors that have been normalized to unity at the top of the building (refer Figure 6). The modal participation factors are presented in for the first three modes of vibration. Eq (4) is hence simplified to:

$$\theta_{ave} = \frac{1.5 \mathbf{RSD}(T_1)}{H} \quad (5)$$

It was found from the parametric studies that the maximum drift in the building typically occurred at the roof level provided that the building is supported by structural walls only or jointly supported by structural walls and moment frames. Therefore, the maximum drift demand from each mode of vibration can be estimated as follow:

$$MAX(\delta_{i,j} - \delta_{i-1,j}) = (\phi_{10,j} - \phi_{9,j}) \mathbf{PF}_j \mathbf{RSD}(T_j) \quad (6)$$

where, $MAX(\delta_{i,j} - \delta_{i-1,j})$ is the maximum drift contributed by the j_{th} mode of vibration, $\phi_{10,j}$ and $\phi_{9,j}$ are the modal displacement at level 10 and 9 of the j_{th} mode of vibration as shown in Figure 6, \mathbf{PF}_j is the participation factor for the j_{th} mode of vibration, $\mathbf{RSD}(T_j)$ is the response spectral displacement at the j_{th} natural period of vibration.

The maximum drift angle $\theta_{max,j}$ attributed to vibration mode j is defined by the following equation:

$$\theta_{max,j} = \frac{(\phi_{10,j} - \phi_{9,j}) \mathbf{PF}_j \mathbf{RSD}(T_j)}{H/10} \quad (7)$$

The values of $(\phi_{10,j} - \phi_{9,j})$ and \mathbf{PF}_j for the first three modes of vibration obtained from parametric studies are presented in Table 3.

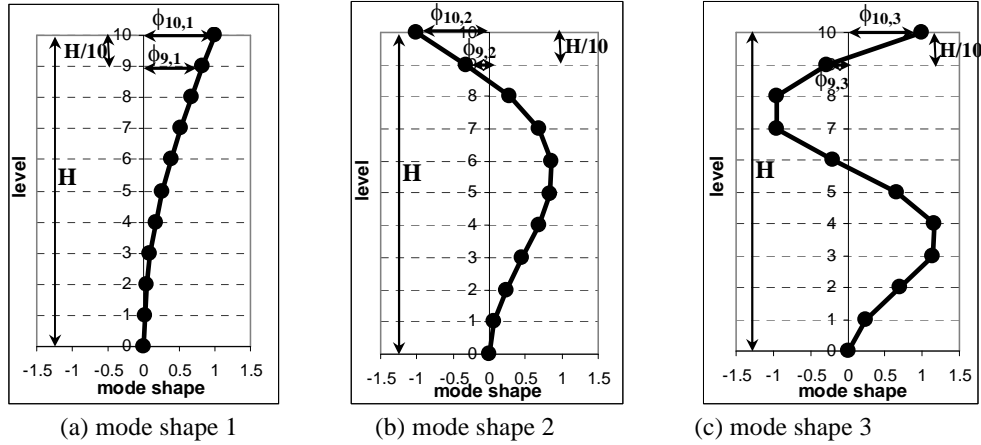


Figure 6 Generic mode shapes of multi-storey buildings

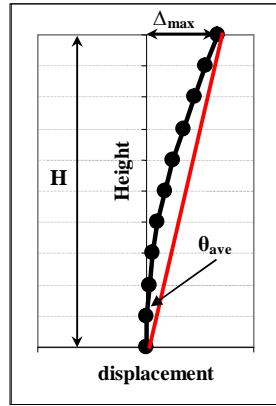


Figure 7 Fundamental mode of vibration of multi-storey buildings

Table 3 Modal displacements and participation factors for three modes of vibration

Mode of vibration	$(\phi_{10,j} - \phi_{9,j})$	PF _j
1	0.16	1.5
2	-0.67	0.72
3	1.28	0.38

Eq (7) can be simplified as follows:

$$\theta_{\max,1} = \frac{2.5 \text{ RSD}(T_1)}{H} \quad \text{for mode 1} \quad (8a)$$

$$\theta_{\max,2} = \frac{-4.9 \text{ RSD}(T_2)}{H} \quad \text{for mode 2} \quad (8b)$$

$$\theta_{\max,3} = \frac{4.7 \text{ RSD}(T_3)}{H} \quad \text{for mode 3} \quad (8c)$$

The drift amplification factor for each mode can be determined by combining Eqs (2), (5) and (8). The maximum drift amplification factor λ_{\max} can be estimated by modal superposition using the “square-root-of-the-sum of the squares” method. The maximum drift amplification factor λ_{\max} is hence defined by the following equation.

$$\lambda_{\max} = \sqrt{(1.64)^2 + (-3.3)^2 (\text{RSD}(T_2)/\text{RSD}(T_1))^2 + (3.15)^2 (\text{RSD}(T_3)/\text{RSD}(T_1))^2} \quad (9)$$

The following expressions can be used to estimate the maximum angle of drift θ_{\max} based on the bi-linear displacement response spectrum model as shown in Figure 8:

$$\theta_{\max} = \lambda_{\max} \frac{1.5 \text{RSD}(T_1)}{H} \quad \text{and,} \quad (10a)$$

for $T_1, T_2, T_3 \leq T_{\text{corner}}$ (Figure 8a):

$$\lambda_{\max} = \sqrt{1.64^2 + 3.3^2 (T_2/T_1)^2 + 3.15^2 (T_3/T_1)^2} \quad (10b)$$

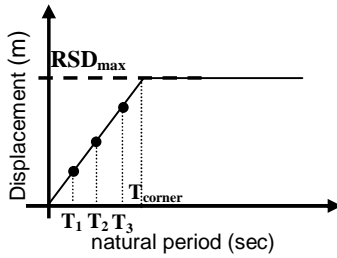
for $T_2, T_3 \leq T_{\text{corner}}$ (Figure 8b):

$$\lambda_{\max} = \sqrt{1.64^2 + 3.3^2 (T_2/T_{\text{corner}})^2 + 3.15^2 (T_3/T_{\text{corner}})^2} \quad (10c)$$

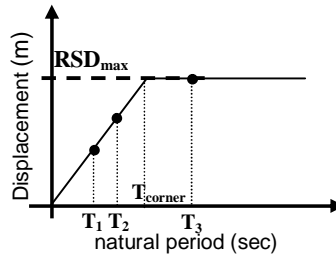
for $T_3 \leq T_{\text{corner}}$ (Figure 8c):

$$\lambda_{\max} = \sqrt{1.64^2 + 3.3^2 + 3.15^2 (T_3/T_{\text{corner}})^2} \quad (10d)$$

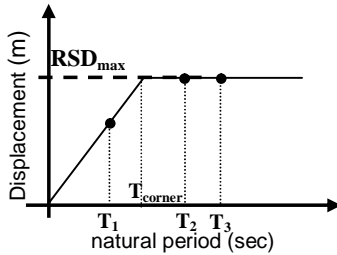
where T_1 , T_2 and T_3 are the first, second and third natural period of vibration respectively. T_{corner} is the second corner period at which the linear part of the response spectrum intercepts the constant (flat) part of the response spectrum. The maximum drift amplification factor λ_{\max} can be conservatively estimated by assuming that all three periods of vibration are on the flat part of the displacement response spectrum (Figure 8d). λ_{\max} can be calculated using Eq(9) with the ratio of $\text{RSD}(T_2)/\text{RSD}(T_1)$ and $\text{RSD}(T_3)/\text{RSD}(T_1)$ equals to 1.0. The value of λ_{\max} was found to be up to about 5.



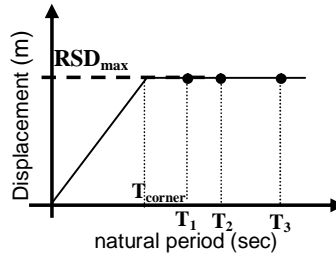
(a) λ_{\max} according to Eq (10b)



(b) λ_{\max} according to Eq (10c)



(c) λ_{\max} according to Eq (10d)



(d) $\lambda_{\max} = 5$

Figure 8 Bi-linear response spectrum

4 Inelastic Drift Demand on Non-ductile Structures

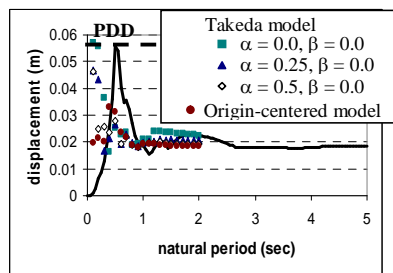
Drift demands of inelastic responding structures can be approximated by results obtained from modal analyses (Section 3.2) if the effects of stiffness and strength degradation are represented in terms of the effective stiffness of the lateral resisting elements (Priestley et al., 2007). It is assumed herein that inelastic actions only occur at the base of the cantilever wall. Thus, only the lateral stiffness at the base of the wall is reduced according to its maximum displacement capacity. As shown in Section 3.1, the distribution of stiffness up the height of the wall has insignificant effects on the modal displacement shapes. Thus, stiffness reduction of the wall resulted from inelastic behaviour would only lengthen the natural period of vibration of the building and not its deflection shape except where there is a soft-storey feature in the building.

Parametric studies have been undertaken on SDOF systems based on non-linear time history analyses of non-ductile structures (Lumantarna et al., 2009). It was found from the studies that the well known *equal-displacement* proposition can provide a reasonable estimate of the maximum displacement demand of systems in the displacement sensitive regions (ie. $T > T_{\text{corner}}$). However, there are uncertainties associated with the displacement demand on systems in the acceleration and velocity controlled regions (ie. $T < T_{\text{corner}}$). Importantly, the maximum inelastic displacement demands (represented by the symbols in Figure 9a) is represented conservatively by the highest point on the displacement response spectrum (**PDD**) (Figure 9a), or the constant part of the response spectrum in the bi-linear form (Figure 9b).

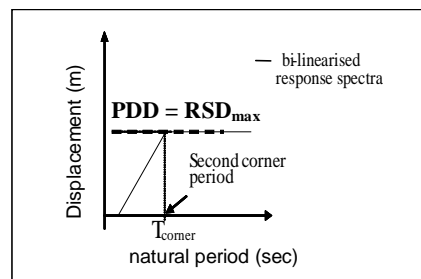
By assuming a constant displacement demand, the maximum drift demand on the building can be conservatively estimated by applying an amplification factor of 5 to the average drift demand. Thus, the maximum drift demand (θ_{max}) of inelastic responding structures can be estimated by the simple expression:

$$\theta_{\text{max}} = 5 \theta_{\text{ave}} \quad \text{and} \quad \theta_{\text{ave}} = \frac{1.5 \text{ PDD}}{H} \quad (11)$$

PDD is equal to RSD_{max} and H is the total height of the building.



(a) Inelastic displacement demands of SDOF (subject to generated earthquake)



(b) PDD on bi-linearised response spectrum

Figure 9 Inelastic maximum displacement demand of non-ductile structures

5 Prediction of Drift Demand

Seismic assessment of structures in regions of low to moderate seismicity can be based on comparison of the drift demand on the structure with drift capacity. The maximum drift demand in tall buildings can be estimated as follow:

$$\theta_{\max} = \frac{7.5 \text{ PDD}}{H} \quad (12)$$

where, PDD is the maximum displacement demand of non-ductile structures and H is the height of the building. The maximum displacement demand **PDD** can be estimated as follow:

$$\text{PDD} = \text{RSD}_{\max} \quad (12a)$$

where RSD_{\max} is the maximum response spectral displacement.

The maximum drift demand on a tall building could be estimated using the proposed approach. A building of 50 m in height and is laterally supported by a combination of shear walls and moment resisting frames has its maximum drift demand estimated using Eq (12) and along with values of RSD_{\max} listed in Table 1. The drift demands so estimated for different site classes and levels of seismic hazard as per AS1170.4 (2007) are summarised in Table 4.

Table 4 Estimates of θ_{\max} (%) for Australian conditions

Site	500 yr RP ($k_p = 1.0$)				2500 yr RP ($k_p = 1.8$)			
	Z = 0.06	Z = 0.08	Z = 0.10	Z = 0.12	Z = 0.06	Z = 0.08	Z = 0.10	Z = 0.12
Class B	0.3	0.4	0.5	0.6	0.5	0.7	0.9	1.1
Class C	0.4	0.5	0.7	0.8	0.7	1.0	1.2	1.5
Class D	0.7	0.9	1.1	1.3	1.2	1.6	2.0	2.4
Class E	1.0	1.4	1.7	2.0	1.8	2.4	3.0	3.7

The maximum drift demands can be compared to the ultimate drift limit of 1.5% as stipulated by AS1170.4 (2007). It is shown that the maximum drift demands are mostly within the stipulated drift limits except for the most onerous site conditions. Thus buildings considered in this study could generally be deemed safe when subject to the level of ground shaking stipulated by the standard for a return period of 500 – 2500 years.

6 Concluding Remarks

This paper presents interim findings from a research which is aimed at producing estimates of the drift demands in tall buildings. Parametric studies were undertaken on multi-storey buildings which were of varying height and were supported by the combined actions of moment frames and shear walls in varying proportions. It was found that the shape of deflection in the significant vibration modes of a tall building was not sensitive to its height. The maximum drift demand on the building can be estimated in accordance with the identified generic mode shapes. The maximum drift demand on the building can be conservatively estimated by the use of a simple expression in which an amplification factor of 5 is applied to the calculated average drift demand (ie. $\theta_{\max}=5 \theta_{\text{ave}}$, where $\theta_{\text{ave}}=1.5 \text{ PDD}/H$). A quick assessment of the potential state of damage to the building can be obtained by comparing the maximum drift demand to the ultimate drift limit.

7 References

- AS 1170.4 2007. *Structural Design Actions – Part 4 Earthquake Actions*. Sydney: Standards Australia.
- AS/NZS 1170.2 2002. *Structural Design Actions – Part 2 Wind Actions*. Sydney: Standards Australia.
- Bhamare, R., Wibowo, A., Wilson, J., Gad, E., Lam, N. 2008. Seismic Performance Assessment of Soft-Storey Buildings Based on Results from Field Testing. *20th Australasian Conference on the Mechanics of Structures and Materials*, Towoomba, Australia.
- Lam, N., Wilson, J., Lumantarna, E. 2009. Simulations of Seismically Induced Storey-Drift in Buildings. *Journal of Structural Engineering and Mechanics*, in review.
- Lam, N & Chandler, A. 2005. Peak displacement demand of small to moderate magnitude earthquake in stable continental regions, *Earthquake Engineering and Structural Dynamics* 34: 1047-1072.
- Lam, N., Wilson, J., Chandler, A. & Hutchinson, G. 2000. Response spectrum modeling for rock sites in low and moderate seismicity regions combining velocity, displacement and acceleration predictions, *Earthquake Engineering and Structural Dynamics* 29: 1491-1525.
- Lumantarna, E., Lam, N., Wilson, J, Griffith, M. 2009. Inelastic Displacement Demand of Strength Degraded Structures, *Journal of Earthquake Engineering*, in press.
- Lumantarna, E., Bhamare, R., Lam, N., Wilson, J. 2007. Displacement Controlled Behaviour of Structures subject to Moderate Ground Shaking. *Australian Earthquake Engineering Society Conference 2007*, Wollongong, NSW.
- Lumantarna, E., Lam, N., Kafle, B., Wilson, J. 2008. Displacement Controlled Behaviour of Asymmetrical Buildings. *Australian Earthquake Engineering Society Conference 2008*, Ballarat, Vic.
- Priestley, M. J. N., Calvi, G. M. and Kowalsky, M. J. 2007. *Displacement-Based Seismic Design of Structures*, IUSS PRESS, Pavia.